Astron. Astrophys. 364, 660–664 (2000)

ASTRONOMY AND ASTROPHYSICS

The distribution of calcium on the surface of ϵ Ursae Majoris: an abundance distribution Doppler image

D.E. Holmgren and J.B. Rice

Brandon University, Department of Physics & Astronomy, Brandon, Manitoba, R7A 6A9 Canada (holmgren,rice@brandonu.ca)

Received 19 July 2000 / Accepted 8 September 2000

Abstract. We present a surface abundance Doppler image of singly–ionized calcium for the Bp star ϵ UMa based on high signal-to-noise CCD spectra. This map shows striking similarities to that of oxygen (Rice et al. 1997) and perhaps iron (Rice & Wehlau 1990). The Ca II 866.2 nm line has allowed us to obtain a detailed surface abundance map of calcium for ϵ UMa. The calcium abundance map has been used to locate the position of the positive magnetic pole on ϵ UMa at a longitude of 350.8 deg and a latitude of 25.8 deg. Calcium is distributed in a ring along the magnetic equator, along which the abundance is $[Ca/H] = -5$, which is close to a normal population I value. This represents an enhancement with respect to other regions by a factor of $\sim 10^3$. A secondary feature is present with $[Ca/H] = -6.5$. A chemically differentiated stellar wind is proposed as the main mechanism for generating the surface abundance distribution of calcium.

Key words: stars: abundances – stars: chemically peculiar – stars: individual: ϵ UMa

1. Introduction

The chemically peculiar B star ϵ Ursae Majoris (HD112185,HR 4905) is one of the archetypal objects of its class: those stars showing line profile variability due to surface abundance variations, possibly in addition to variability caused by a surface magnetic field. ϵ UMa is certainly the most widely–studied Ap star, and several surface abundance Doppler images have been produced (Wehlau et al. 1982; Rice & Wehlau 1990; Donati 1990; Rice & Wehlau 1991; Hatzes 1991). Rice et al. (1997) present a succinct review of previous work on ϵ UMa. Most of the published Doppler images relate to iron, oxygen, or chromium abundances. To our knowledge, only one other map based on singly-ionized calcium has been produced (Babel et al. 1995), and in this case the Ca II K 393.36 nm line was used. However, this map is based on fewer spectra than the map to be presented here. This dearth of Ca maps is most likely due to the fact that the calcium lines are often blended with Balmer or Paschen lines, thus presenting a difficulty in terms of extracting the Ca II line itself. We present here a new map of calcium for ϵ UMa based on the Ca II 860.7 nm line, which we have extracted from the core of the nearby Paschen line. This is followed by a discussion of the calcium surface abundance distribution and its relationship to the surface distributions of other elements. Finally, we consider the implications of our results for elemental diffusion theories.

Send offprint requests to: D.E. Holmgren

2. Observations and reductions

The spectra of ϵ UMa were obtained with the 1.2m telescope of the Dominion Astrophysical Observatory in May 1997. The UBC 4096 CCD was used in conjunction with the 9681 coudé spectrograph (Richardson, 1968) in three wavelength regions: 867.0 nm, 777.5 nm, and 616.0 nm. This spectrograph configuration gives a reciprocal dispersion of 0.5 nm mm^{-1}. The first wavelength region contains the Ca II 866.2 nm line, and we therefore restrict our attention to this region. Analyses and Doppler images for lines in the other regions will be presented in later papers. Exposure times for the 867.0 nm region spectra were 200s per frame. The stellar exposures were obtained in groups of three, and later the spectra in each group were co–added to achieve a higher signal-to-noise ratio. Each series of stellar exposures was bracketed by arc line exposures, and since multiple wavelength regions were observed on a given night, each series of stellar exposure was accompanied by its own set of flat-field exposures. Bias frames were obtained at the start and end of each night. The dates and phases for the co-added spectra are shown in Table 1, where the phases have been computed using the ephemeris of Provin (1953). Also shown in Table 1 are continuum signal–to–noise ratios for each spectrum.

All spectra were reduced using the MIDAS software package (November 1995 version). For each stellar spectrum, mean flat-fields were formed, and were suitably normalized so as to remove only the pixel-to-pixel variations from the stellar data. Wavelength calibration was carried out for each arc spectrum and then interpolated onto the stellar data. At this point, all spectra were exported from MIDAS in FITS format, so that they could be rectified using the SPEFO program (Škoda 1996). We note here that SPEFO allows interactive spectrum rectification using Hermite spline interpolation.

Table 1. ϵ UMa dates, phases, and SNRs

File	HJD	Phase	Phase (deg)	S/N
av8053-57	50582.7405	0.9704	349.3	360
av8123-6	50583.8911	0.1965	70.7	206
av8170-3	50583.8761	0.1936	69.7	120
av8220-3	50584.7008	0.3556	128.0	193
av8274-8	50584.8091	0.3769	135.7	372
av8324-8	50584.8890	0.3926	141.3	222
av8375-9	50584.9633	0.4072	146.6	195
av8412-6	50585.7097	0.5539	199.4	181
av8490-4	50585.8368	0.5789	208.4	218
av8541-5	50585.9083	0.5929	213.5	223
av8627-31	50586.7201	0.7524	270.9	356
av8688-92	50586.8118	0.7705	277.4	309
av8740-4	50586.9111	0.7900	284.4	255
av8791-5	50586.9861	0.8047	289.7	201
av8838-42	50587.7124	0.9475	341.1	190
av8898-02	50587.8138	0.9674	348.3	231
av8949-53	50587.9055	0.9854	354.7	172
av9000-4	50587.9839	0.0008	0.3	270

2.1. Extraction of the Ca II 866.2 nm line

As shown in Fig. 1, the Ca II 866.2 nm line is severely blended with a hydrogen line of the Paschen series. To use this Ca II line for Doppler imaging, it must be extracted from the Paschen line (we refer the reader to Fig. 1 for the following discussion). This was done by first taking one spectrum (av8053-57) and using spline interpolation to remove the Ca II line, effectively leaving the Paschen line profile (the middle profile in Fig. 1). This gave us a time–independent "template" to be divided into other spectra. For most of the spectra, this worked very well, and the residual spectrum was used as input for our Doppler imaging program. However, two spectra near phase 0.0 required special treatment, as the Ca II line is extremely weak near this phase. To extract the Ca II in this case, spline rectification was used to remove the blue wing of the Paschen line, thus leaving the Ca II line. This procedure proved to be much more satisfactory than the division process. All calculations relating to the extraction of the Ca II line were done using the DIPSO program (Howarth et al. 1997).

3. Doppler imaging

The Ca II line profiles recovered by the extraction process just described were used as input for the MAPPER3 Doppler imaging program. The general principles underlying MAPPER3 are discussed by Piskunov & Rice (1993). It should be noted here that the spectrograph instrumental profile was *not* removed through the use of Fourier filtering, as in earlier studies (Rice et al. 1997). The current version of MAPPER3 allows for the convolution of the instrumental profile with the computed stellar line profiles, and it is these which are compared to the observed (input) profiles.

The adopted stellar parameters for ϵ UMa used in the Doppler imaging are shown in Table 2.

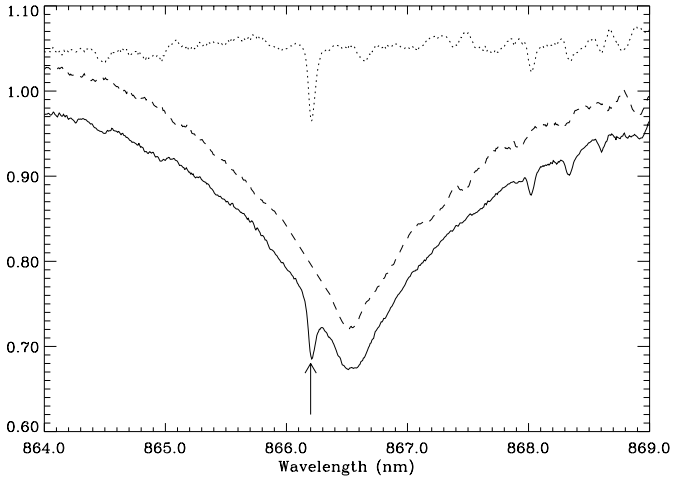

Fig. 1. Extraction of Ca II 866.2 nm from the Paschen line. The bottom profile (solid line) denotes the original data, with the arrow indicating the position of the Ca II line. The middle profile (dashed line) is spectrum 8053-57 with the Ca II line removed. The top profile (dotted line) is the result of the division of these two profiles.

Table 2. Adopted stellar parameters for ϵ UMa

Parameter	value
$T_{\rm eff}$	9500 K
$\log g$ (cgs)	3.5
$v \sin i$	33 km s^{-1}
Inclination i	50 deg
Rotation period	5.0887 d
Microturbulence	1.5 km s^{-1}
Macroturbulence	0.0 km s^{-1}
Radius	4.3 solar

The calcium line used in the imaging has a wavelength of 866.2140 nm, $\log gf = -0.73$, and an excitation potential of 1.692 eV.

For the imaging runs, Tikhonov regularization was used and MAPPER3 was allowed to run for 150 iterations, after which there was clearly very little change in the output Doppler map, and a correspondingly small change in the sum of squares.

The final Doppler images for the Ca II 866.2 nm line are shown in Fig. 2 (spherical projection). The observed and computed line profiles are shown in Fig. 3. We discuss the line profiles and MAPPER's fit to them in the next section.

4. The Doppler image

The Doppler image for singly-ionized calcium is quite similar to that for neutral oxygen published by Rice et al. (1997). An overabundant "band" is located at the magnetic equator, and the rest of the star appears to be relatively underabundant. Note here that we are talking about relative abundance over the stellar surface; the calcium abundance in the band is fairly normal for a population I star. However, there is a feature near the magnetic pole which is clearly different from anything seen on the oxygen map. As it is roughly Y–shaped, we shall refer to it as

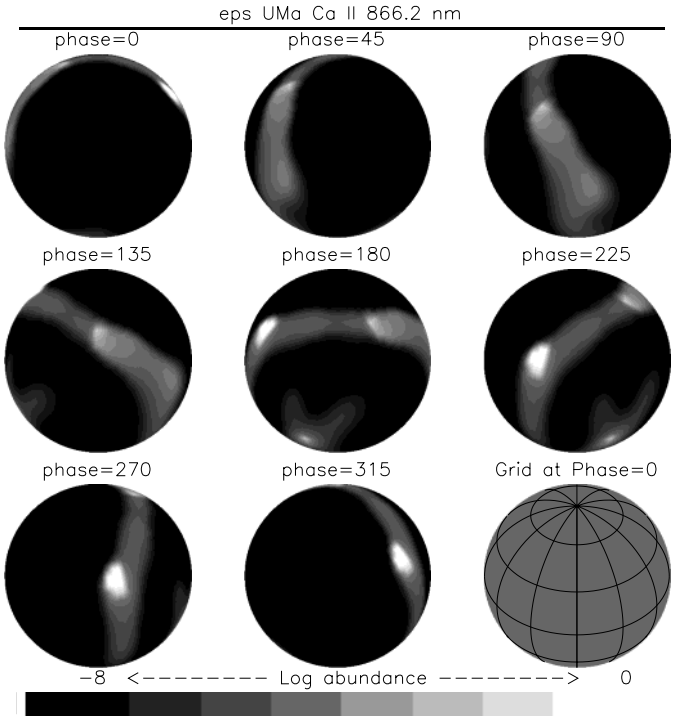

Fig. 2. ϵ UMa Ca II doppler image

the "Y-feature". There is a further similarity to the oxygen map: a spot of overabundance at about the same latitude as the magnetic pole. The Ca II map of Babel et al. (1995) shows only the overabundant ring.

The Y–feature can be traced in the observed profiles, and from this we can conclude that this feature is not an artifact of the imaging algorithm. If one looks at the time sequence of profiles (Fig. 3) and the sequence of spherical projections (Fig. 2), the appearance of the Y–feature is coincident with the profiles having a broad, and in some cases flat–topped appearance. We are referring to phases 128.0 deg through 213.5 deg. When this feature goes beyond the observer's horizon, the profile immediately becomes more peaked as only the spot and ring are visible.

There is a sequence of phases (341 deg through 355 deg) at which the Ca II line is very weak, and the fit found by MAPPER is not as good as it is at other phases. At these phases, the observer is looking at the positive magnetic pole, at which there is very little Ca II visible, and hence the absorption line is very weak. It is thus not surprising that MAPPER's fit at these phases is rather poor.

A Doppler image of ϵ UMa based on the chromium–iron–calcium blend at 452.6 nm is presented by Lüftinger (2000). We find little similarity between our Doppler image and that of Lüftinger. This may be due to the fact that the latter image is based a line blend, which introduces uncertainty in the imaging. Moreover, our map is consistent with the results of Babel et al. (1995) and the oxygen map of Rice et al. (1997). Furthermore, our map is based on data obtained at a higher resolution than that used by Lüftinger.

4.1. Location of the axis of symmetry

Since the axis of symmetry of the Doppler image seems to be connected with the location of magnetic pole (Bohlender & Landstreet 1990), we can infer that the axis of symmetry defines the location of the magnetic pole. We refer the reader to the Mercator projection of the Doppler image in Fig. 4 during the following discussion. By a taking slice through the map in constant latitude, we obtain an abundance profile in longitude. Taking the latitude to be zero, we obtain the profile shown in the top panel of Fig. 5. In this panel, the arrow indicates a blended peak due to the Y–feature. The other two peaks, at longitudes of ~ 80 deg and ~ 250 deg are due to the ring feature. By measuring the locations of these two peaks and then finding their midpoint (170.8 deg), we have that the longitude of the positive magnetic pole is approximately 350.8 deg. The same result is obtained if we demand that the negative pole lie at ± 90 deg from either of these two peaks. Similarly, by taking a latitude slice at a longitude of 180 deg, we obtain the abundance profile in the bottom panel of Fig. 5. Requiring that the negative pole lie 90 deg from the maximum of the latitude profile means that its latitude must be about -25.8 deg. This translates into a latitude of 25.8 deg for the positive pole. To summarize, the location of the positive magnetic pole determined from the Ca II map is at a longitude of 350.8 deg and a latitude of 25.8 deg. According to Rice et al. (1997), the pole latitude and longitude found from the O I map are 349 deg and 28 deg, respectively. Clearly, the locations of the axis of symmetry found from the two maps are in very good agreement.

5. Interpretation of the Doppler image

The new Ca II map presented here can be understood as a result which is intermediate between the maps for oxygen and chromium presented in Rice et al. (1997). Indeed, given that calcium is a metal of intermediate weight, between those of oxygen and chromium, one might expect such a result. The Y–feature can be understood in this way, as can the overabundant "spot" on the ring. Rice et al. (1997) discuss the relative merits of mechanisms that induce abundance variations on the surfaces of Ap stars. They conclude that a chemically differentiated stellar wind is largely responsible for the distribution of neutral oxygen on the surface of ϵ UMa, with little contribution from horizontal radiative acceleration. It would seem that the same mechanism (more-or-less) is operating for Ca II as for oxygen, but the fact that a heavier element is involved may be responsible for the Y–feature. In the case of calcium, the differentiated wind may not be as efficient as it is for oxygen, but nevertheless it has the same effect. Also, there is perhaps a greater contribution from horizontal accelerations, which produces the "Y–feature".

6. Summary

The Ca II 866.2 nm line has allowed us to obtain a detailed surface abundance map of calcium for ϵ UMa. This map is qualitatively similar to that for neutral oxygen, but with some important differences due to the fact that calcium is a somewhat

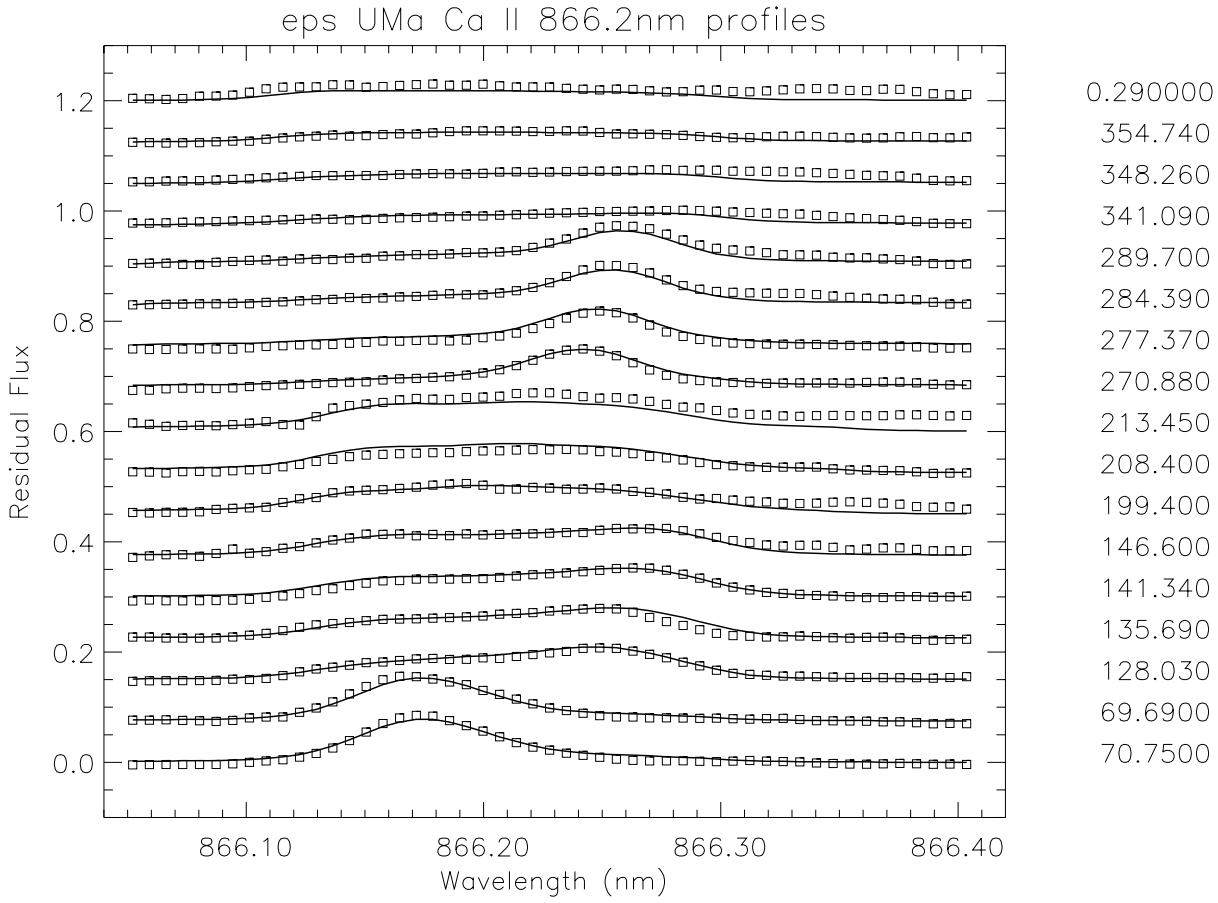

Fig. 3. ϵ UMa Ca II line profiles. Boxes denote the observed profiles, lines the computed ones. The phase of each observation in degrees is on the right hand side of the plot

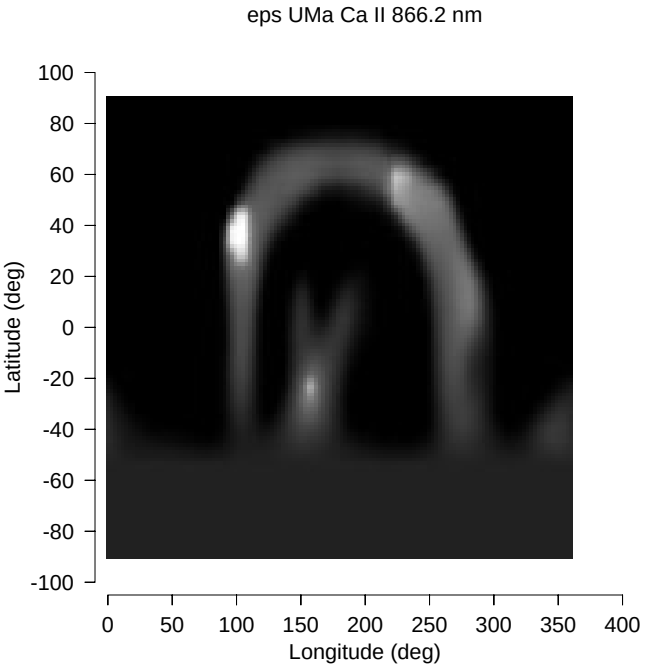

Fig. 4. A Mercator plot of the Ca II Doppler image. Abundance levels are as in Fig. 2. Note that the surface of the star below a latitude of about −50 deg is not visible to the observer

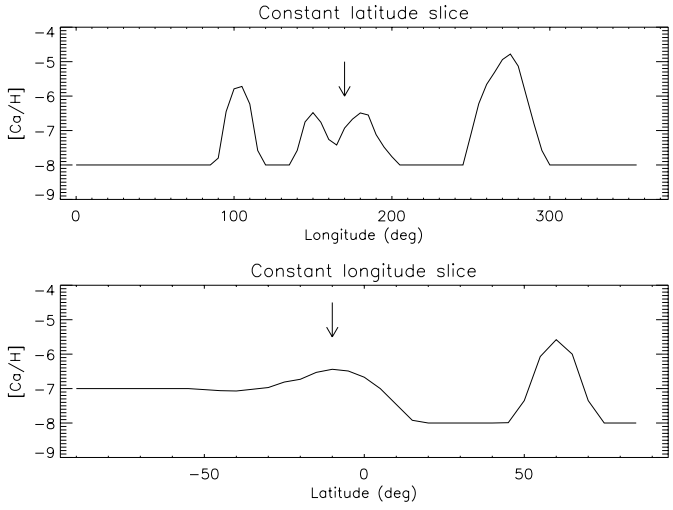

Fig. 5. How to find the location of the magnetic pole. The upper panel is a longitude profile, and the lower a latitude profile. In both panels, the arrow indicates the position of the Y–feature

heavier element. This can be understood as radiative acceleration not being as effective at removing calcium from the surface.

The calcium abundance map has been used to locate the position of the positive magnetic pole on ϵ UMa at a longitude of 350.8 deg and a latitude of 25.8 deg, in good agreement with determinations from other maps.

Calcium is distributed in a ring along the magnetic equator, along which the abundance is $[Ca/H] = -5$, which is close to a normal population I value. This represents an enhancement with respect to other regions by a factor of $\sim 10^3$. A secondary feature is present with $[Ca/H] = -6.5$.

As with neutral oxygen, a chemically differentiated stellar wind is proposed as the main mechanism for generating the surface abundance distribution of calcium. However, there may be as well a contribution from horizontal radiative acceleration in producing some of the details seen on the Ca II Doppler image.

Acknowledgements. We wish to thank an anonymous referee for constructive comments. The authors also wish to thank the director of the Dominion Astrophysical Observatory for a generous allocation of observing time. This project was supported by a NSERC grant to J.B. Rice.

References

Babel J., Donati J.-F., Gonzalez J.-F., 1995, In: Strassmeier K.G. (ed.) Stellar Surface Structure. Poster Proceedings, IAU Sym. 176
Bohlender D.A., Landstreet J.D., 1990, ApJ 358, L25
Donati J.-F., Semel M., del Toro Iniestia J.C., 1990, A&A 233, L17
Hatzes A.P., 1991, MNRAS 253, 89
Howarth I.D., Murray J., Mills D., Berry D.S., 1997, Starlink User Note 50.20, Starlink Project, Rutherford Appleton Laboratory
Lüftinger, T., 2000, Diploma Thesis, University of Vienna
Piskunov N.E., Rice J.B., 1993, PASP 105, 1415
Provin S.S., 1953, ApJ 118, 489
Rice J.B., Wehlau W.H., 1990, A&A 233, 503
Rice J.B., Wehlau W.H., 1991, A&A 246, 195
Rice J.B., Wehlau W.H., Holmgren D.E., 1997, A&A 326, 988
Richardson E.H., 1968, J. R. Astron. Soc. Can. 62, 313
Škoda P., 1996, In: Jacoby G.H., Barnes J. (eds.) Astronomical Data Analysis Software and Systems V, ASP Conference Series Vol. 101, ASP, San Francisco, p. 187
Wehlau W., Rice J., Piskunov N., Khokhlova V., 1982, Pis'ma Astron. Zh. 8, 30